A necroptosis-related lncRNA signature can accurately predict the survival outcome of bladder cancer patients

Zhifang Ma (zhifangma@163.com)
First Hospital of Shanxi Medical University
Wei Zhang
Shanxi Medical University
Wei Wang
Second Hospital of Shanxi Medical University
Shen Wang
First Hospital of Shanxi Medical University
Liying Song
Shanxi Medical University
Zhaoyu Ren
Shanxi Medical University
Zhongyuan Bai
Shanxi Medical University
Fang Wang
First Hospital of Shanxi Medical University
Ruijie Zhao
First Hospital of Shanxi Medical University
Yaran Gao
Shenyang Agricultural University

Research Article

Keywords: lncRNA, bladder cancer, necroptosis, TCGA

Posted Date: March 14th, 2022

DOI: https://doi.org/10.21203/rs.3.rs-1441832/v1

Abstract

Bladder cancer is the second most common malignant tumor in the male genitourinary system. This study explored the prognostic role of necroptosis-related long noncoding RNAs (LncRNAs) in bladder cancer.We used univariate Cox, least absolute shrinkage and selection operator and multivariate Cox regression models to establish a necroptosis-related lncRNA prognostic signature. Then, 13 necroptosis-related lncRNAs were included in risk signature. Patients were divided into the high- and low-risk group based on the median risk score. The risk signature predicted that the areas under the receiver operating characteristic curve of patients at 1 year, 3 years and 5 years were 0.74, 0.78 and 0.79, respectively. Next, nomograms and correction curves were established using risk signature and clinicopathological factors. The nomogram-corrected curve shows a good fit. Gene Set Enrichment Analysis was used to explore the possible molecular mechanisms underlying the different prognosis of the low-risk and high-risk of patients, and showed that tumor-related signaling pathways and intercellular connectivity-related signaling pathways were significantly enriched in the high-risk group, while metabolism-related pathways were enriched in the low-risk group. In addition, Immune cell infiltration analysis and was performed on the two groups of patients and the response to immunotherapy was judged. Finally, tumor mutation data were analyzed, and potentially sensitive chemotherapy drugs were screened. The low-risk group was more sensitive to methotrexate while the patients in the high-risk group were more sensitive to cisplatin, docetaxel, paclitaxel and thapsigargin.

Background

Bladder cancer (BC) is the fourth most common cancer in men and second only to prostate cancer in the genitourinary system, of which 90% is of the urothelial type. Also,80% are non-muscle invasive[1]. According to the 2018 Global Cancer Statistics, there were about 549,000 new cases of BC and 200,000 died each year[2]. Because of the limited accuracy of pathological staging in predicting BC survival[3], in recent years, many researchers have turned their attention to molecular biomarkers. Therefore, it is particularly important to establish an accurate and predictive molecular biomarker to guide the selection of chemotherapy, radiotherapy, and immunotherapy for different patients and to accurately judge the prognosis.

Necroptosis is a new programmed cell death way different from apoptosis, mainly composed of RIPK1 (receptor interacting protein kinase 1), RIPK3 (receptor interacting protein kinase 3) and MLKL (mixed lineage kinase domain-like pseudokinase) mediated [4, 5]. Necroptosis was also found to be involved in the maintenance of T cell homeostasis[6], because necroptosis has been indicated to clear up excessive and abnormal T cells in the absence of caspase-8[7], which is considered to aid apoptosis by acting as the major machinery countering the abnormal proliferation of lymphocytes[8]. Many studies have shown that necroptosis played an important role in tumorigenesis[9], progression, metastasis[10]and response to immunotherapy [11, 12].

LncRNA (long non-coding RNA) is a non-coding RNA of more than 200 nucleotides. It plays an important role in multiple steps of the gene expression process, including: chromatin, transcription, post-transcription. In cell differentiation, cell cycle regulation, stem cell pluripotency and many biological processes[13–16], numerous studies have reported that it occupied an important position in tumorigenesis and development[3, 17]. In BC, the lncRNAs PEG10, LINC01614 and ADAMTS9-AS1 promoted cell survival, invasion and migration[18–20]. LncRNA TUG1 promoted BC metastasis[21]. Also, LncRNAs were closely linked to a variety of programmed cell death including apoptosis, autophagy, and necroptosis[22, 23]. It was found that the necroptosis-related LncRNA prognostic model could accurately predict the prognosis of gastric cancer patients and help to distinguish hot tumors from cold tumors[24]. Our study established a stable prognostic model to guide clinical practice by exploring the relationship between necroptosis-related LncRNA and the prognosis of BC patients.

Meterial And Methods

Patients and datasets

TCGA was used to obtain the RNA sequence data and clinical information of BC. Expression and clinical information (including age, gender, stage, and prognosis) for RNA-seq (including mRNAs and lncRNAs) were obtained from TCGA database (https://portal.gdc.cancer.gov/). Patients with survival time less than 30 days were excluded. Finally, 396 cases were incorporated into our study. The necroptosis-related gene sets was downloaded from GSEA (http://www.gsea-msigdb.org): GOBP_NECROPTOTIC_SIGNALING_PATHWAY (M24779), and others necroptosis-related genes reported in recent studies, including a total of 67 genes(supplementary table1). Since data of participants were acquired from the public database, written informed consent and approval of the ethics committee were waived.

Identification of necroptosis-associated lncRNAs

The‘limma’ package was used in the R software to calculate Pearson correlation coefficients, which

were employed to analyze the correlation between necroptosis hallmark genes and lncRNAs in TCGA dataset. The necroptosis-related lncRNAs with absolute value of correlation coefficient greater than 0.3 (|R|>0.6) and P value less than 0.05 ($P < 0.05$) were screened out and used to construct the necroptosis-related signature[5].

Construction of the prognostic-related necroptosis lncRNA signature

We conducted univariate Cox regression analysis, least absolute shrinkage and selection operator (LASSO) regression analysis, and multivariate Cox regression analysis to evaluate their prognostic value. Then, based on the above results, we selected the most representative candidates through LASSO analysis. Subsequently, these lncRNAs associated with survival were subjected to multivariate Cox

regression analysis to construct the BC prognostic model. Moreover, on the basis of the median risk score, the patients were classified into one high-risk group and the other low-risk group.

$$riskscore = \sum_{i=1}^{n} coefficient_i * EXPlncRNA_i$$

Regression coefficients for each lncRNA obtained through multivariate regression analysis.

Assessment of necroptosis-related lncRNA signatures

The risk score of each sample is calculated according to the above formula. If the risk score of the sample is greater than the median of all sample risk scores, it is a high-risk group, otherwise it is a low-risk group The Kaplan–Meier method was used to compare overall survival (OS) of patients in different risk groups. 3D principle component analysis (PCA) was used to evaluate the distribution of genes expression in patients with different risk levels. Stratified survival analysis was performed to examine the accuracy and stability of the necroptosis lncRNAs signature.

Nomogram construction and validation.

Age, gender, stage, grade, and necroptosis-related risk score were incorporated into the univariate Cox regression analysis and multivariate Cox regression analysis, and then ROC curves

were used to evaluate the predictive accuracy of the risk score and other clinicopathological parameters. After that, we picked up the independent predictive factors with $P < 0.05$ to build a Cox regression model and presented it with a nomogram to facilitate clinical practice. Then a corrected curve was used to compare the difference between the true survival rate and the predicted survival rate to reflect the accuracy of the predictive model.

Gene set enrichment analysis (GSEA)

We uploaded the patient's RNA-seq expression profile and patient grouping information to GSEA, and conducted Kyoto Encyclopedia of Genes and Genomes (KEGG) pathway analysis to explain the differential signaling pathways of BCpatients between the high-risk group and the low-risk group, thus deriving their biological functions. Using GSEA version 4.2.1, the threshold for judging enriched pathways was $FDR < 0.25$, $P < 0.05$.

Immune infiltration analysis,

The CIBERSORT tool was used to analyze the composition of each patient's 22 immune cells, and the Wilcoxon test was used to compare the composition of each immune cell between high-risk and low-risk patients.

Predict immune response

To predict differences in response to immunotherapy between different risk profile groups, potential immune marker genes PD-1, PD-L1, and mismatch repair genes (MLH1, MSH2, MSH6, and PMS2) were

identified between high and low-risk groups. The expression levels between the two groups were used for comparison. Finally, we used The Cancer Immunome Atlas (TCIA) database (https://tcia.at/) to generate the immunophenoscore (IPS) in each sample, which was a superior predictor of response to anti-cytotoxic T lymphocyte antigen-4 (CTLA-4) and anti-programmed cell death protein 1 (PD-1), and then the IPS in different risk groups were compared to explore the relationships between risk scores and IPS. $P < 0.05$ was considered statistically significant.

Tumor mutation analysis

The tumor mutation burden of each sample was calculated from the tumor mutation data and compared between the high and low-risk groups. The mutation data was analyzed by the maftools R package to compare the differences in mutated genes between the two groups.

Drug screening

Public Pharmacogenomics Database Genomics of Cancer Drug Sensitivity (GDSC) was used to evaluate and predict chemotherapy response in BC patients with different risk groups in the TCGA database, and the half-maximal inhibitory concentration (IC50) of chemotherapy drugs for BC was used to evaluate and predict chemotherapy in high and low-risk groups. Through comparison between groups, chemotherapy drugs suitable for patients in different risk groups were selected, and Wilcoxon signed rank test was used for evaluation, and $P < 0.05$ was considered to be statistically significant.

Statistical analysis

All of the statistical analyses in our study were performed using R version 4.1.0. We evaluated the correlation through Pearson correlation analysis and constructed survival curves through Kaplan–Meier analysis. Univariate and multivariate Cox regression analyses were utilized to examine the independence of our prognostic risk model in predicting the prognosis of BC patients. The ROC curve was used to assess our model's accuracy in predicting BC patient survival.

Results

Identification of necroptosis-related lncRNAs and construction of a risk score model.

We obtained a total of 67 necroptosis genes by summarizing the GSEA gene set and genes reported by other studies. The patient genetic data were split through the gencode.v22 annotation file obtained from TCGA website to obtain an expression matrix containing 14,805 LncRNAs and 19,712 mRNAs respectively, and then 970 necroptosis-related lncRNAs were obtained. Univariate Cox regression analysis showed that the expression of 78 LncRNAs were tightly associated with overall survival in BC patients, and the screening threshold was $P < 0.01$. In order to prevent overfitting of the model, the above genes were included in the LASSO regression analysis, and a total of 25 genes (Fig. 1a-b) were obtained. Finally, the LASSO results were included in the multivariate cox regression analysis, and 13 lncRNAs were obtained as "RP11_111K18.2" " RP11_262A16.1", "RP11_446N19.1", "NR2F2_AS1" "LINC_PINT"

"CTD_2027I19.3", "RP11_291B21.2" "USP30_AS1", "RP5_1184F4.5", "AC006160.5", "DLEU1_AS1" "_SLC25A25", "RP11_385D13.3" (Fig. 1c), and the results were used to construct a risk signature.

Assessment of risk models

The patients were divided into high-risk group and low-risk group according to the median of risk score, and K-M survival analysis was used to compare the prognosis of the two groups of patients. Overall, survival time was significantly shorter in the high-risk group compared to the low-risk group (Fig. 2a). The risk scores of the high-risk and low-risk groups are shown in Fig. 2b. As the patients risk score increased, the patients mortality was higher (Fig. 2c). the expressions of RP11-262A16.1, NR2F2-AS1, RP11-385D13.3 and DLEU1-AS1 increased notably with the increment of risk scores, while the expressions of others lncRNAs decreased distinctly, which were in accordance with hazard ratio of these predictors(Fig. 2d). 3D principal component analysis using all necroptosis-related lncRNAs and risk signature lncRNAs clearly showed that our risk signature can distinguish the two groups of patients well (Fig. 2e-f). To predict the accuracy of the risk model for predicting overall survival, time ROC curves were used to assess and the areas under the 1-year, 3-year, and 5-year ROC curves were 0.74, 0.78, and 0.79, respectively (Fig. 2g). To verify the stability of the risk profile, we combined information from TCGA patients and age (≤ 65 vs > 65), sex (male vs female), pathological grade (low-grade vs high-grade), pathological stage (stagel- II vs stage III-IV), T stage (T1-2 vs T3-4), and N stage (N0 vs N1-3) were stratified to compare the survival rates of patients in high and low-risk groups. The K-M survival curve showed that the patients in ≤ 65 ($P < 0.0001$), > 65 ($P < 0.0001$), male ($P < 0.0001$), female ($P = 0.00024$), stage III-IV ($P = 0.00067$), pathologically high grade ($P = 0.00024$). $P < 0.0001$), T3-4 ($P = 0.00041$), N0 ($P < 0.0001$), and N1-3 ($P = 0.00013$) subgroups had significantly higher survival rates in the low-risk group than in the high-risk group, but in stage I -II ($P = 0.22$), T1-2 ($P = 0.23$) and low pathological grade ($P = 1$) subgroup, the difference was no significance (Fig. 3). To test the applicability for predictions of overall survival based on all TCGA patient data sets, 396 patients were randomized into two testing data sets. In the first testing data set, the high-risk patients had a lower overall survival rate than the low-risk group ($P < 0.0001$, Fig. 4a), and the areas under the ROC curve at 1, 3, and 5 years were 0.75, 0.80, and 0.82, respectively (Fig. 4c). In the second testing data set of patients, the overall survival rate of high-risk patients was still lower than that of low-risk patients ($P < 0.0001$, Fig. 4b), and the areas under the ROC curve were0.73, 0.77, and 0.77 at 1 year, 3 years, and 5 years, respectively (Fig. 4d). The results observed in both groups were consistent with those based on all patients, illustrating the applicability of the risk signature.

Independent prognostic analysis and nomogram

In order to explore the independent prognostic factors related to the prognosis of BC patients, the risk signature, age, gender, pathological T stage, and pathological N stage of the patients were included in univariate cox regression and multivariate cox regression. Because there were too many missing data for M staging, it was not included in the analysis. In addition to gender, other factors were associated with overall survival in univariate regression and in multivariate cox regression (Fig. 5a-b). It could be seen that age, pathological T stage, pathological N stage, and risk characteristics were all the independent

prognostic factors of the patient's survival, and nomogram was dawn for the above factors(Fig. 5c), then the correction curve was conducted to compare the difference of predicted survival rate and the real survival rate, and the correction curve showed a good fit (Fig. 5d-f). Then, the risk signature were compared with clinical and pathological factors in the ROC curves and we found that the prediction accuracy of risk signature was the highest (AUC = 0.729), which was higher than that of age (AUC = 0.673), pathological stage (AUC = 0.642), pathological T stage (AUC = 0.615), and pathological N stage (AUC = 0.621) and Gender (AUC = 0.452) respectively (Fig. 5g).

GSEA enrichment analysis

In order to explore the molecular signaling mechanism of the possible role to the risk characteristics established by necroptosis-related lncRNAs leading to different prognosis between the high and low-risk groups, we performed GSEA enrichment analysis of differential expression genes between them. The results of GSEA enrichment analysis showed that tumor-related signaling pathways and some intercellular adhesion pathways were significantly enriched in the high-risk group, including: melanoma, glioma, endometrial cancer, renal cell carcinoma, cancer, BC, colorectal cancer, pancreatic cancer, prostate cancer, basal cell carcinoma, WNT signaling pathway, TGF-β signaling pathway, CALCIUM signaling pathway, MAPK signaling pathway, HEDGEHOG signaling pathway, adhesion junction and tight junction. However, metabolic-related pathways were significantly enriched in the low-risk group, including peroxisomes, and α-linolenic acid metabolism(Fig. 6).

Correlation between risk signature and immune

Twenty-two immune cells were evaluated in the TCGA database, and 9 immune cells were significantly different in high-risk and low-risk groups, including macrophage M0 type, macrophage

M2 type, neutrophils, activated NK cells were significantly elevated in the high-risk group, whereas resting NK cells, plasma cells, naive CD4 T cells, CD8 T cells, regulatory T cells (Tregs) were significantly elevated in the low-risk group (Fig. 7). Since PD-1 (PDCD1), PD-L1 (CD274), Microsatellite instability (MSI), including MLH1, MSH2, MSH6, and PMS2 were frequently used as prognostic markers of immune response, we analyzed the difference of expression between different risk groups. We first analyzed the difference between PD-1 and PD-L1 expression between the two groups, and found that PD-1 and PD-L1 were not significantly different between the high and low-risk groups(Fig. 8a-b). Then we compared MSI-related genes and found that the difference between the high and low-risk groups. Compared with the high-risk group, the expression of MLH1 and MSH2 in the high-risk group were slightly higher, and the expressions of MSH6 and PMS2 were significantly increased ($P < 0.1$, Fig. 8c-f), showed that microsatellites were more stable in the high-risk group. We also explored the relationship between risk score and tumor mutational burden, as high tumor mutational burden (TMB) represented a better response to immunotherapy. TMB showed a significant downward trend with increasing risk score ($R=-0.22$, $P = 7.1e-06$, Fig. 8g). We then deducted a K-M survival analysis, combining risk signature and TMB and patients were divided into high-risk & high-TMB subgroup, high-risk & low-TMB subgroup, high-risk & low-TMB subgroup and low-risk & low-TMB subgroup. It was found that the low-risk and high-TMB

subgroup had the best overall survival, while the high-risk and low-TMB subgroup had the worst overall survival (Fig. 8h). Finally, we used the TCIA database to generate an IPS value for each patient, the IPS value could be a good indicator of the response to anti-PD-1, anti-CTLA-4 drugs. The IPS score of anti-PD-1, anti-CTLA-4 and anti-PD-1 CTLA-4 was significantly lower in the high-risk group than in the low-risk group(Fig. 8I-k), so it could be predicted that patients in the low-risk group would respond better to immunotherapy than the high-risk group. Comprehensive analysis of the above results showed that patients in the high-risk group had a weaker response to immunotherapy than the low-risk group. In order to compare the differentially expressed mutant genes in the two groups, we listed the top 20 highly mutant genes in two group (supplement Fig. 1–2) and finally found that SYNE1 (23% VS 15%, P = 0.041), MACF1 (20% VS 12%, P = 0.042) and FAT4 (19% VS 10%, P = 0.011) were significantly different mutant genes.

Predicting response to chemotherapy drugs

The pRRophetic R package was used to explore the GDSC database to compare whether necroptotic lncRNA signature were used to predict differences in response to chemotherapy between high and low-risk groups. We used chemotherapy drugs commonly used in the treatment of muscle-invasive BC, including gemcitabine, cisplatin, methotrexate, vinblastine, and doxorubicin, and commonly used chemotherapy drugs in the treatment of non-muscle-invasive BC, including camptothecin, docetaxel, paclitaxel and thapsigargin. half maximal inhibitory concentration (IC50) is used to evaluate response to

chemotherapeutic drugs. The IC50 of methotrexate in the high-risk group was significantly higher than that in the low-risk group(Fig. 9a), indicating that methotrexate was sensitive to patients in the low-risk group. The IC50s of cisplatin, docetaxel, paclitaxel and thapsigargin were significantly higher in the low-risk group than in the high-risk group(Fig. 9b,-e), implying that these drugs were sensitive to high-risk patients. However, the other drugs did not differ significantly between the two groups.

Discussion

Among the most common tumors, BC is the tenth most common cancer, and the male-to-female ratio is approximately 3.5 : 1[25]. However, due to the limitations of pathological staging in predicting the prognosis of different patients, it is particularly important to discover a new prognostic feature. Recently, with the advancement of sequencing technology, more and more researchers have begun to explore the prognostic value based on genes. Apoptosis has historically been believed to be the only form of programmed cell death (PCD), and necrosis, which was believed to be an “accidental” type of death not regulated by molecular events[26], was assumed to be the diametrically opposite modality of cell death compared to apoptosis until necroptosis was discovered as a novel programmed form of necrotic cell death that bears a mechanistic resemblance to apoptosis and a morphological resemblance to necrosis[27]. Due to the important role of necroptosis-related lncRNA in the breast cancer, colon cancer and Gastric Cancer[24, 28, 29], we constructed its signature in BC for the first time to predict the prognosis of BC patients.

We constructed a stable prediction signature with 13 genes, including "RP11-111K18.2", "RP11-262A16.1", "RP11-446N19.1", "NR2F2-AS1", "LINC-PINT", "CTD-2027I19.3", "RP11-291B21.2", "USP30-AS1", "RP5-1184F4.5", "AC006160". 5", "DLEU1-AS1", "SLC25A25-AS1", and "RP11-385D13.3", the areas under the ROC curve of 1 year, 3 years and 5 years were 0.73, 0.79 and 0.80, respectively. According to multiple factors ROC curve, the areas of risk signature was higher than that of age (0.673), pathological stage (0.642), pathological T stage (0.615), pathological N stage (0.621) and Gender (0.452) respectively. Next, we made a prediction model with the risk characteristics, T stage, N stage, and age, and displayed it with a nomogram. The correction curve showed that the prediction model could accurately predict the true survival rate. We further validated the robustness of the risk model in clinicopathological subgroups, the judgment of overall survival rate was no significance in the low clinical stage (P = 0.22), low T stage (P = 0.23), and low pathological grade (P = 1) subgroups due to the limitation of sample size, other subgroups could make significant distinctions, showing the accuracy of the model. We randomized 396 patients into two testing data sets and the overall survival rate of high-risk patients was lower than that of low-risk patients in both testing data sets. It illustrated the applicability of our risk signature.

We analyzed each gene in the risk signature, NR2F2-AS1 induced epithelial-mesenchymal transition in non-small cell lung cancer, promoted prostate cancer cell proliferation by regulating CDK4, and modulated the MAPK pathway to regulate colorectal cancer invasion and metastasis[30–32]. LINC-PINT inhibited the proliferation and migration of laryngeal squamous cell carcinoma by silencing ZEB1[33], and it can also inhibited the invasiveness of thyroid cancer by downregulating miR-767-5p to induce TET2 expression[34]. USP30-AS1 acted as a ferroptosis-related LncRNA signature to predict the prognosis of BC patients[35]. Li Y's study showed that down-regulation of SLC25A25-AS1 promoted the proliferation of colorectal cancer cells and was resistant to chemotherapy[36]. The other lncRNA included in our signature have not been explored, which will be researched in the future studies by our group.

We performed GSEA enrichment analysis on genes in high and low risk groups, and found that cancer-related pathways and some intercellular adhesion pathways were significantly enriched in high risk groups. The HEDGEHOG signaling pathway was considered to play an important role in the occurrence of BC tumor stem cells[37]. The WNT signaling pathway and the MAPK signaling pathway played an important role in the invasion and spread of BC tissues[38, 39], TGF-β signaling pathway had been implicated in the occurrence of various human diseases including malignant tumors[40]. Paxillin enabled breast tumor invasion by maintaining adherens junctions[41]. Xu X's study showed that the tight junction protein ZONAB was upregulated in BC cell lines and promoted BC invasion[42], indicating that this high-risk group had a poor prognosis. However, metabolic-related pathways were significantly enriched in the low-risk group. Such as peroxisomes, reactive oxygen species could be produced in peroxisomes, elevated ROS production efficiently inhibited chemo-drug resistance and promoted chemoresistant cell death[43], and α-linolenic acid intake has a protective effect on the development of BC[44].

We explored the relationship between immune cell infiltration and necroptosis-related LncRNAs and found that the risk level of BC patients may be potentially affected by immune infiltration. In recent years, more and more researchers had paid attention to the immunotherapy. The clinical impact of checkpoint

blockade strategies, providing a survival advantage compared with traditional chemotherapies, had grown considerably, and had been tested in various tumors including melanoma, renal cell carcinoma, non-small cell lung cancer, and urothelial carcinoma over the past several decades. Phase III clinical trial illustrated that pembrolizumab was associated with a lower rate of treatment-related adverse events and with significantly longer OS than chemotherapy as a second-line therapy for platinum-refractory advanced urothelial carcinoma[45]. However, the expression of immune checkpoints was not significantly different between high-risk and low-risk groups. Recent work suggests that MSI may be used as a predictor for immune-checkpoint blockade therapy. Several clinical studies have shown better outcomes among patients with MSI-positive tumors as compared to negative groups when they are treated with inhibitors of programmed cell death 1 (PD-1)[46, 47]. In our study, the microsatellite status was more stable in the high-risk group, so the low-risk group were more effective to immunotherapy, consistented with our risk characteristics predictions.

Finally, we used risk signature to predict patient response to chemotherapy drugs. The low-risk group were more sensitive to methotrexate. In contrast, patients in the high-risk group were more sensitive to cisplatin, docetaxel, paclitaxel and thapsigargin. Taken together, our necroptosis-associated lncRNA signature could accurately predict chemotherapy response in patients with BC, which may be helpful for clinical medical decision-making.

The Thirteen-gene prognostic model can effectively predict the prognosis of patients with BC and may provide a clinical setting for individualized treatment of BC in the future. However, it should be pointed out that this study had some limitations: First, since development and validation of the signature in our study was based on TCGA database, it has not been verified in large-scale clinical samples, which may lead to selection bias. Secondly, biochemical experiments such as quantitative real-time PCR, immunohistochemistry, and flow cytometry must be designed to authenticate our model and further clarify the mechanism by which necroptosis-related lncRNAs regulate the pathological process of BC.

Conclusions

This was the first necroptosis-related lncRNA signature in BC, which could accurately predict the overall survival in patients with BC compared with the traditional pathological parameters. Moreover, the molecular signature had close relationships with some certain infiltrating immune cells, and mutational genes in tumors. More verifications will be required in future to validate the stability and practicability of the present signature.

Declarations

Acknowledgments

We would like to thank Bioinfor-Medical Centre for excellent technical assistance.

Authors’ contributions

Study concept and design: WZ, WW, ZM, and LS. Acquisition of the data: WZ, WW, SW and ZR. Analysis and interpretation of the data: WZ, WW, SW and YG. Drafting of the manuscript: WZ, WW, FW and LS. Statistical analysis: WZ, WW, ZB, RZ and ZM. Technical support: WZ, WW and LS. All the authors read and approved the final manuscript.

Conflict of interest

The authors declare no conflicts of interest.

Ethical approval

Not required to this study.

Consent to participate

Not required to this study.

Consent for publication

Not required.

References

1. Berdik, C., *Unlocking bladder cancer.* Nature, 2017. **551**(7679): p. S34-S35.
2. Bray, F., et al., *Global cancer statistics 2018: GLOBOCAN estimates of incidence and mortality worldwide for 36 cancers in 185 countries.* CA: a cancer journal for clinicians, 2018. **68**(6): p. 394-424.
3. Sun, Z., et al., *An autophagy-related long non-coding RNA prognostic signature accurately predicts survival outcomes in bladder urothelial carcinoma patients.* Aging, 2020. **12**(15): p. 15624-15637.
4. Zhang, Z., *Predictive analytics in the era of big data: opportunities and challenges.* Annals of translational medicine, 2020. **8**(4): p. 68.
5. Degterev, A., et al., *Identification of RIP1 kinase as a specific cellular target of necrostatins.* Nature chemical biology, 2008. **4**(5): p. 313-321.
6. Kaczmarek, A., P. Vandenabeele, and D.V. Krysko, *Necroptosis: the release of damage-associated molecular patterns and its physiological relevance.* Immunity, 2013. **38**(2): p. 209-223.

7. Ch'en, I.L., et al., *Mechanisms of necroptosis in T cells.* The Journal of experimental medicine, 2011. **208**(4): p. 633-641.
8. Lenardo, M., et al., *Mature T lymphocyte apoptosis–immune regulation in a dynamic and unpredictable antigenic environment.* Annual review of immunology, 1999. **17**: p. 221-253.
9. Ghandi, M., et al., *Next-generation characterization of the Cancer Cell Line Encyclopedia.* Nature, 2019. **569**(7757): p. 503-508.
10. Jiao, D., et al., *Necroptosis of tumor cells leads to tumor necrosis and promotes tumor metastasis.* Cell research, 2018. **28**(8): p. 868-870.
11. Yatim, N., et al., *RIPK1 and NF-κB signaling in dying cells determines cross-priming of CD8 T cells.* Science (New York, N.Y.), 2015. **350**(6258): p. 328-334.
12. Aaes, T.L., et al., *Vaccination with Necroptotic Cancer Cells Induces Efficient Anti-tumor Immunity.* Cell reports, 2016. **15**(2): p. 274-287.
13. Wang, J., et al., *LncRNA HOXA-AS2 and its molecular mechanisms in human cancer.* Clinica chimica acta; international journal of clinical chemistry, 2018. **485**: p. 229-233.
14. Yang, Z., et al., *LncRNA: Shedding light on mechanisms and opportunities in fibrosis and aging.* Ageing research reviews, 2019. **52**: p. 17-31.
15. Liao, K., et al., *The research progress of LncRNA involved in the regulation of inflammatory diseases.* Molecular immunology, 2018. **101**: p. 182-188.
16. Bhan, A., M. Soleimani, and S.S. Mandal, *Long Noncoding RNA and Cancer: A New Paradigm.* Cancer research, 2017. **77**(15): p. 3965-3981.
17. Quan, J., et al., *LncRNA as a diagnostic and prognostic biomarker in bladder cancer: a systematic review and meta-analysis.* OncoTargets and therapy, 2018. **11**: p. 6415-6424.
18. Jiang, F., et al., *Retraction notice to "lncRNA PEG10 promotes cell survival, invasion and migration by sponging miR-134 in human bladder cancer" [Biomed. Pharmacother. 114 (2019) 108814].* Biomedicine & pharmacotherapy = Biomedecine & pharmacotherapie, 2022. **145**: p. 112511.
19. Wang, Z., et al., *Novel lncRNA LINC01614 Facilitates Bladder Cancer Proliferation, Migration and Invasion Through the miR-217/RUNX2/Wnt/β-Catenin Axis.* Cancer management and research, 2021. **13**: p. 8387-8397.
20. Yang, G., et al., *lncRNA ADAMTS9-AS1 promotes bladder cancer cell invasion, migration, and inhibits apoptosis and autophagy through PI3K/AKT/mTOR signaling pathway.* The international journal of biochemistry & cell biology, 2021. **140**: p. 106069.
21. Tan, J., et al., *LncRNA TUG1 promotes bladder cancer malignant behaviors by regulating the miR-320a/FOXQ1 axis.* Cellular signalling, 2022. **91**: p. 110216.
22. Tao, H., et al., *LncRNA MEG3 inhibits trophoblast invasion and trophoblast-mediated VSMC loss in uterine spiral artery remodeling.* Molecular reproduction and development, 2019. **86**(6): p. 686-695.
23. Xiong, H., et al., *LncRNA HULC triggers autophagy via stabilizing Sirt1 and attenuates the chemosensitivity of HCC cells.* Oncogene, 2017. **36**(25): p. 3528-3540.

24. Zhao, Z., et al., *Necroptosis-Related lncRNAs: Predicting Prognosis and the Distinction between the Cold and Hot Tumors in Gastric Cancer.* Journal of oncology, 2021. **2021**: p. 6718443.
25. Ferlay, J., et al., *Cancer incidence and mortality worldwide: sources, methods and major patterns in GLOBOCAN 2012.* International journal of cancer, 2015. **136**(5): p. E359-E386.
26. Linkermann, A. and D.R. Green, *Necroptosis.* The New England journal of medicine, 2014. **370**(5): p. 455-465.
27. Christofferson, D.E. and J. Yuan, *Necroptosis as an alternative form of programmed cell death.* Current opinion in cell biology, 2010. **22**(2): p. 263-268.
28. Chen, F., et al., *Necroptosis-related lncRNA to establish novel prognostic signature and predict the immunotherapy response in breast cancer.* Journal of clinical laboratory analysis, 2022: p. e24302.
29. Liu, L., et al., *Comprehensive Analysis of Necroptosis-Related Long Noncoding RNA Immune Infiltration and Prediction of Prognosis in Patients With Colon Cancer.* Frontiers in molecular biosciences, 2022. **9**: p. 811269.
30. Liu, C., et al., *LncRNA NR2F2-AS1 induces epithelial-mesenchymal transition of non-small cell lung cancer by modulating BVR/ATF-2 pathway via regulating miR-545-5p/c-Met axis.* American journal of cancer research, 2021. **11**(10): p. 4844-4865.
31. Fu, X., et al., *LncRNA NR2F2-AS1 positively regulates CDK4 to promote cancer cell proliferation in prostate carcinoma.* The aging male : the official journal of the International Society for the Study of the Aging Male, 2020. **23**(5): p. 1073-1079.
32. Liu, S., et al., *The miR-106b/NR2F2-AS1/PLEKHO2 Axis Regulates Migration and Invasion of Colorectal Cancer through the MAPK Pathway.* International journal of molecular sciences, 2021. **22**(11).
33. Yang, X., et al., *LncRNA LINC-PINT Inhibits Malignant Behaviors of Laryngeal Squamous Cell Carcinoma Cells via Inhibiting ZEB1.* Pathology oncology research : POR, 2021. **27**: p. 584466.
34. Jia, M., et al., *LINC-PINT Suppresses the Aggressiveness of Thyroid Cancer by Downregulating miR-767-5p to Induce TET2 Expression.* Molecular therapy. Nucleic acids, 2020. **22**: p. 319-328.
35. Cui, Y., et al., *Identification of a Nomogram from Ferroptosis-Related Long Noncoding RNAs Signature to Analyze Overall Survival in Patients with Bladder Cancer.* Journal of oncology, 2021. **2021**: p. 8533464.
36. Li, Y., et al., *Decreased expression of LncRNA SLC25A25-AS1 promotes proliferation, chemoresistance, and EMT in colorectal cancer cells.* Tumour biology : the journal of the International Society for Oncodevelopmental Biology and Medicine, 2016. **37**(10): p. 14205-14215.
37. Li, C., et al., *GALNT1-Mediated Glycosylation and Activation of Sonic Hedgehog Signaling Maintains the Self-Renewal and Tumor-Initiating Capacity of Bladder Cancer Stem Cells.* Cancer research, 2016. **76**(5): p. 1273-1283.
38. Chen, Z., et al., *RSPO3 promotes the aggressiveness of bladder cancer via Wnt/β-catenin and Hedgehog signaling pathways.* Carcinogenesis, 2019. **40**(2): p. 360-369.

39. Qiu, D., Y. Zhu, and Z. Cong, *YAP Triggers Bladder Cancer Proliferation by Affecting the MAPK Pathway.* Cancer management and research, 2020. **12**: p. 12205-12214.
40. Massagué, J., S.W. Blain, and R.S. Lo, *TGFbeta signaling in growth control, cancer, and heritable disorders.* Cell, 2000. **103**(2): p. 295-309.
41. Xu, W., et al., *Paxillin promotes breast tumor collective cell invasion through maintenance of adherens junction integrity.* Molecular biology of the cell, 2022. **33**(2): p. ar14.
42. Xu, X., K. You, and B. Wu, *Zonula occludens-1 associated nucleic acid binding protein plays an invasion-promoting role in bladder cancer.* Neoplasma, 2019. **66**(3): p. 405-419.
43. Xu, X., et al., *Enhanced Intracellular Reactive Oxygen Species by Photodynamic Therapy Effectively Promotes Chemoresistant Cell Death.* International journal of biological sciences, 2022. **18**(1): p. 374-385.
44. Brinkman, M.T., et al., *Intake of α-linolenic acid and other fatty acids in relation to the risk of bladder cancer: results from the New Hampshire case-control study.* The British journal of nutrition, 2011. **106**(7): p. 1070-1077.
45. Bellmunt, J., et al., *Pembrolizumab as Second-Line Therapy for Advanced Urothelial Carcinoma.* The New England journal of medicine, 2017. **376**(11): p. 1015-1026.
46. Le, D.T., et al., *PD-1 Blockade in Tumors with Mismatch-Repair Deficiency.* The New England journal of medicine, 2015. **372**(26): p. 2509-2520.
47. Timmermann, B., et al., *Somatic mutation profiles of MSI and MSS colorectal cancer identified by whole exome next generation sequencing and bioinformatics analysis.* PloS one, 2010. **5**(12): p. e15661.

Figures

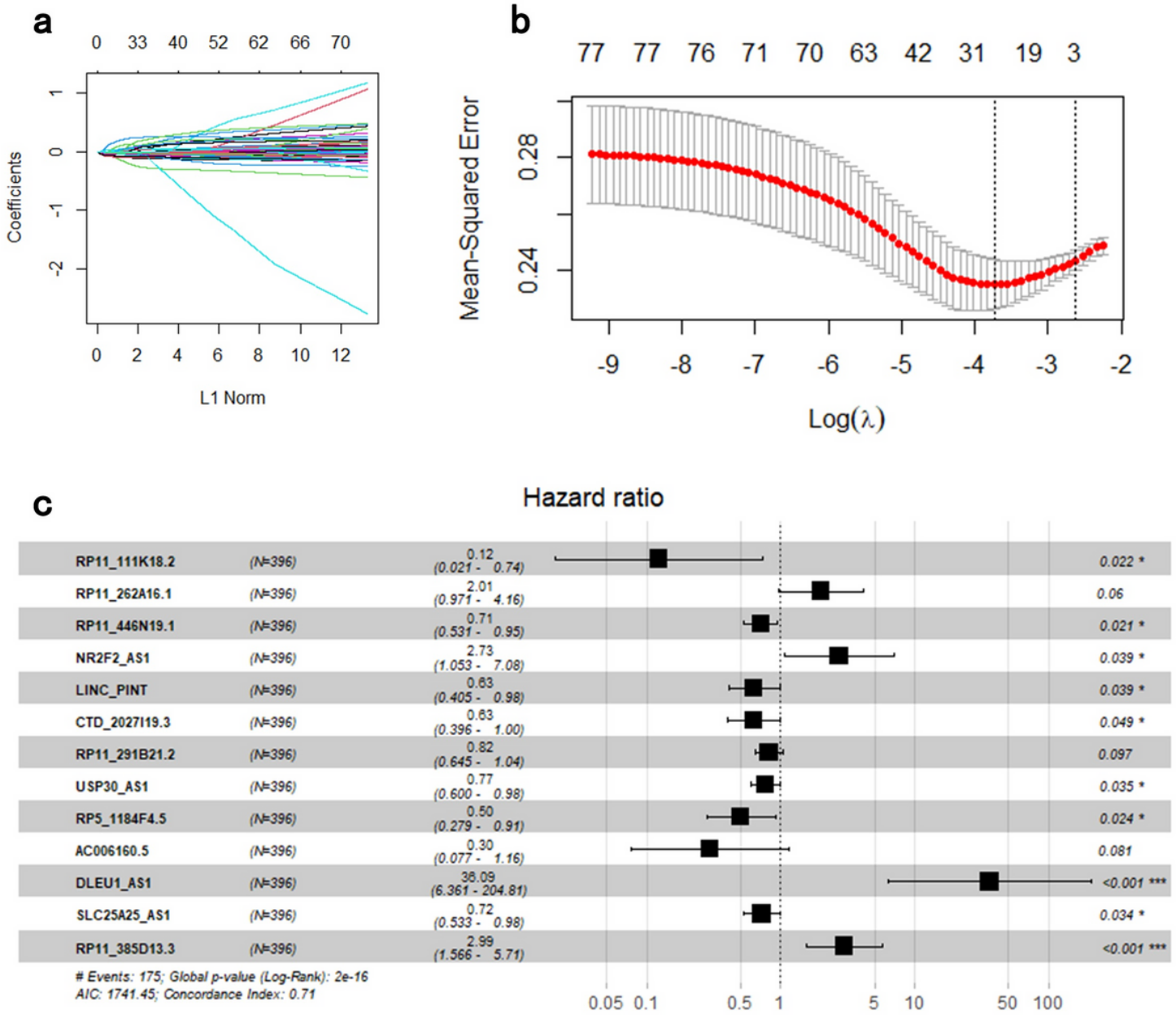

Figure 1

The selection of necroptosis-related lncRNA utilizing Lasso regression analysis. (a,b) The prognosis-related necroptosis lncRNAs screened by univariate Cox regression were incorporated into Lasso regression analysis. Penalty parameter (λ) for the model was determined by 10-fold cross-validation following the criteria that error is within 1 standard error of the minimum. (c) Thirteen prognosis related necroptosis genes were incorporated into multivariate regression model. *P < 0.05; **P < 0.01; *** P < 0.001; ns: no significance.

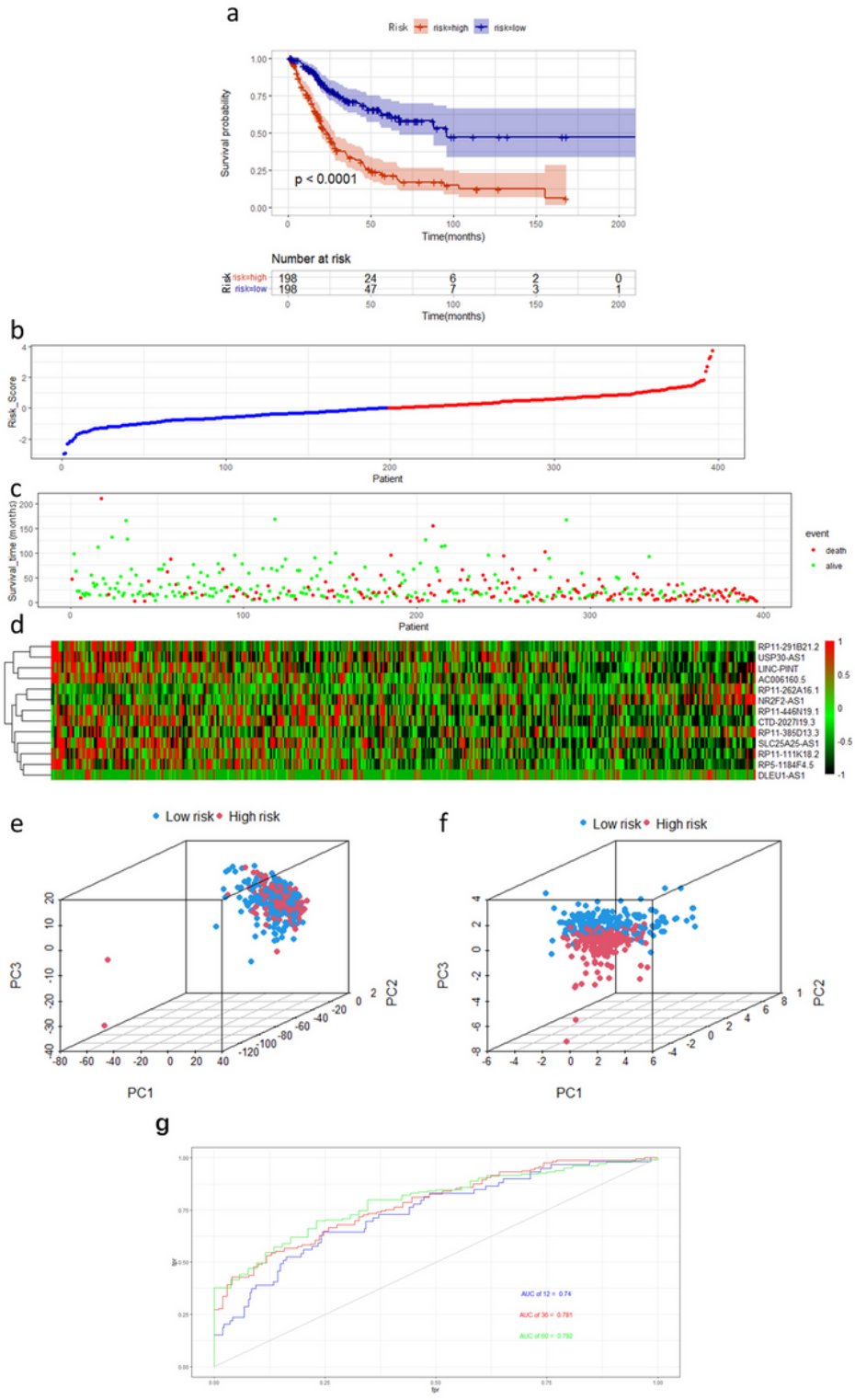

Figure 2

Construction a necroptosis-associated prognostic lncRNA signature. (a) Kaplan–Meier analysis showed that the overall survival of patients in the low-risk groups were longer than those in the high-risk groups in the TCGA database. (b) Distribution of patients with different risk scores based on the necroptosis-related lncRNA prognostic signature. (c) Scatter plot showed that patients with lower risk scores had better survival and lower. (d)Heatmap of the necroptosis lncRNA signature showed that RP11-

111K18.2,AC006160.5,RP5-1184F4.5,CTD-2027I19.3,LINC-PINT,RP11-446N19.1,SLC25A25-AS1,USP30-AS1 and RP11-291B21.2 decreased notably with the increment of risk scores, while the expressions of RP11-262A16.1, NR2F2-AS1, RP11-385D13.3 and DLEU1-AS1 increased distinctly. (e,f) Principal components analysis based on the necroptosis lncRNAs signature demonstrated that two distinctly different distribution patterns between high-risk and low-risk groups. (g) The areas under the 1-year, 3-year, and 5-year ROC curves. ROC, receiver operating characteristic; TCGA, The Cancer Genome Atlas.

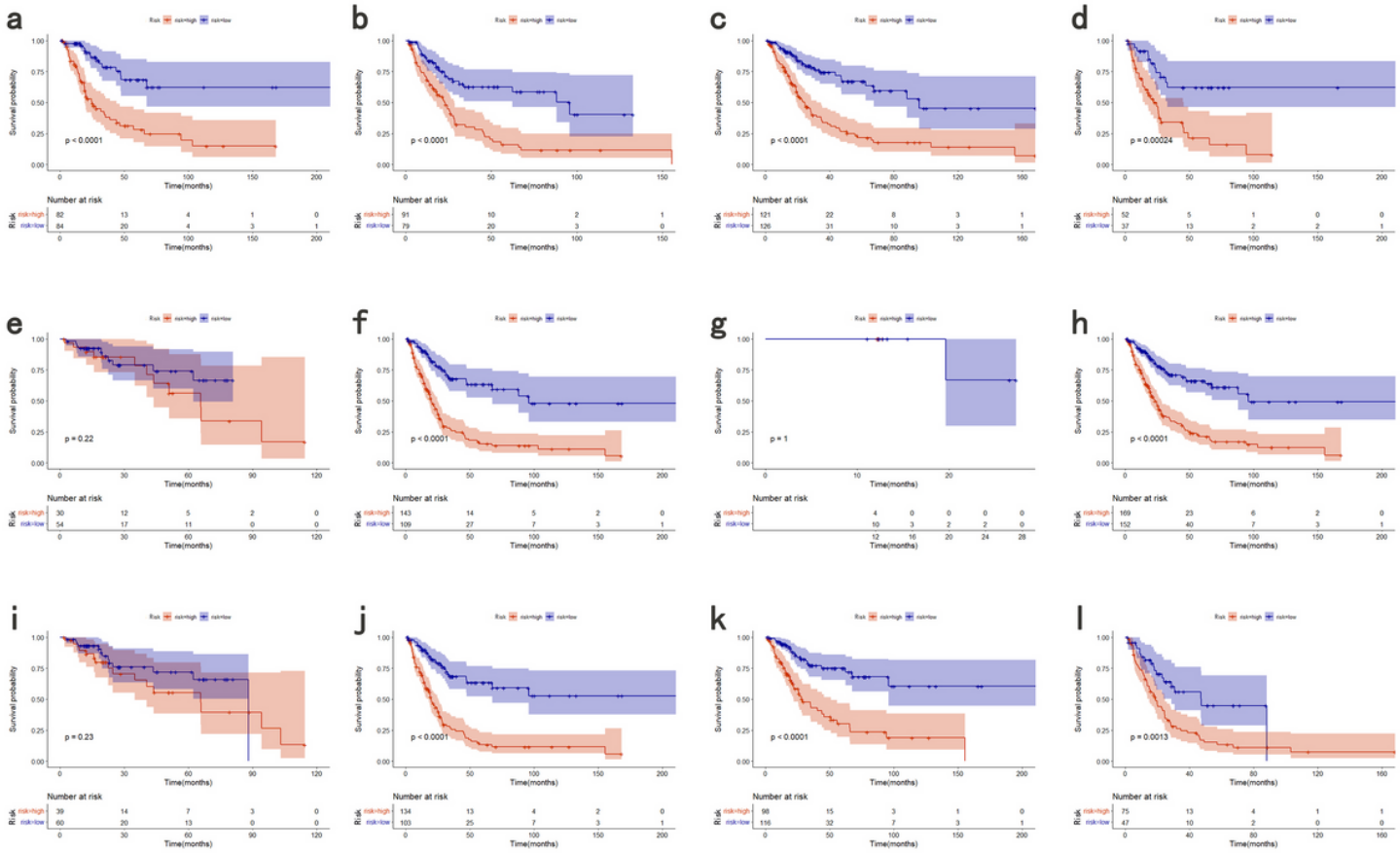

Figure 3

The Kaplan–Meier analysis showed that bladder cancer patients with lower risk scores still had better OS than the ones with higher risk scores in subgroups of age≤65(a), age≥ 65 (b), male (c),female (d), high AJCC-stage (f), high pathological grade (h), high T-stage (j), nodal metastasis-free (k) and nodal metastasis (l), While the difference of OS was not significant in the subgroups of low AJCC-stage (e), low pathological grade (g) and low T-stage (i). OS, overall survival.

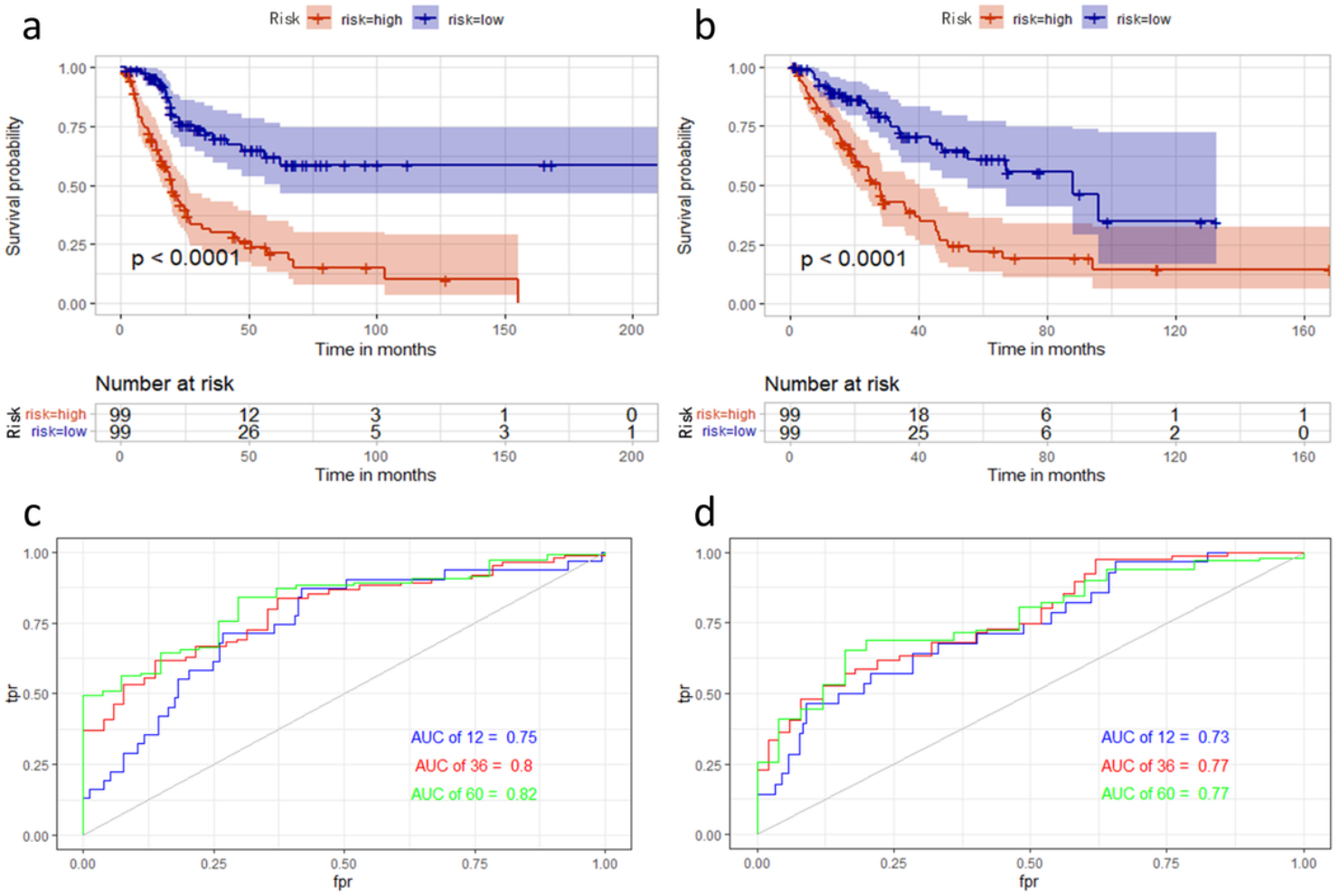

Figure 4

Validation of the predictive signature for OS based on the entire TCGA dataset. (A) Kaplan-Meier survival curve in the first testing cohort. (B) Kaplan-Meier survival curve in the second testing cohort. (C) ROC curve and AUCs at 1-year, 3-years and 5-years survival in the first testing cohort. (D) ROC curve and AUCs at 1-year, 3-years and 5-years survival in the second testing cohort. ROC, receiver operating characteristic; AUC, area under the curve; TCGA, The Cancer Genome Atlas.

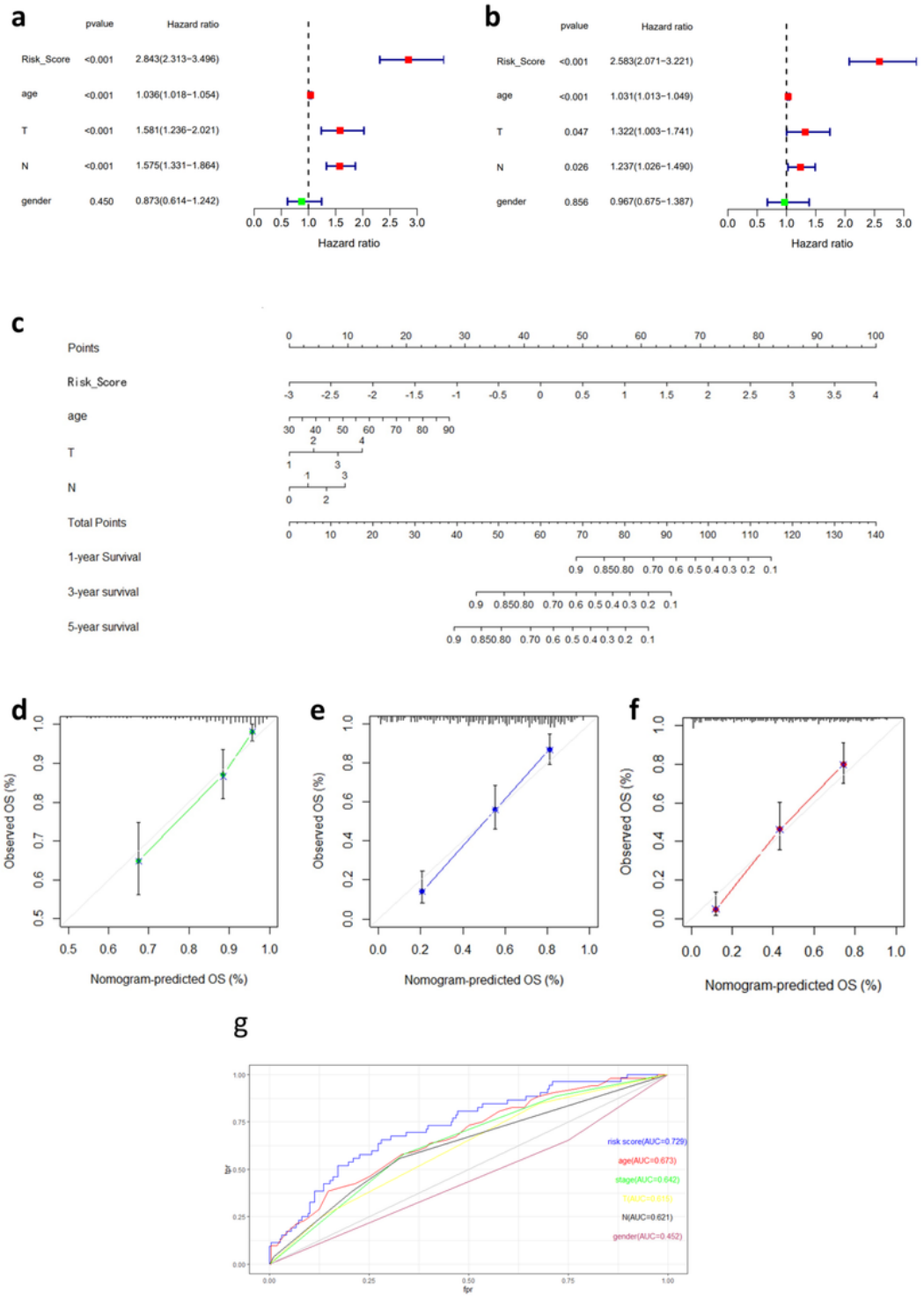

Figure 5

Correlation of the necroptosis-related lncRNA signatures with clinical features (a) Univariate Cox regression analysis and (b)multivariate Cox regression analysis were applied to inspect whether the necroptosis-related lncRNA prognostic signature was independent of age, T, N and gender. (c) A nomogram combining clinicopathological parameters and risk score predicts 1, 3, and 5 years OS of BC patients. (d-f) The calibration curves test consistency between the actual OS rates and the predicted

survival rates at 1, 3 and 5 years. N, lymph node; OS, overall survival. (g)The multiple ROC curves of the risk score and other clinicopathological parameters demonstrated the excellent discrimination of the risk score based on necroptosis lncRNA signature.

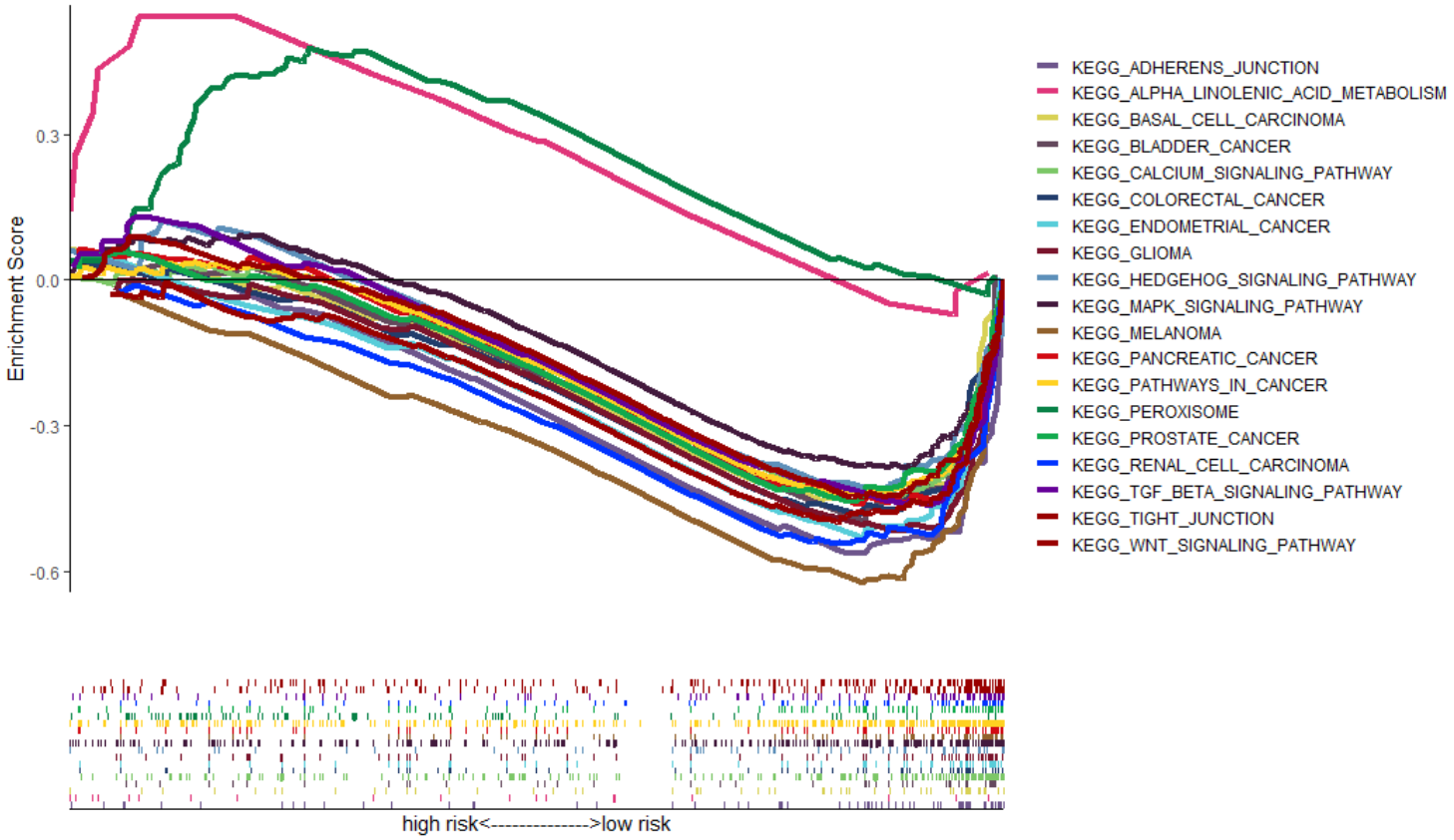

Figure 6

Multiple GSEA pathways in the high-risk and low-risk groups. GSEA results showed that significant enrichment of cancer-related signaling pathways and intercellular adhesion pathways in the high-risk group, but significant enrichment of metabolism-related signaling pathways in the low-risk group.

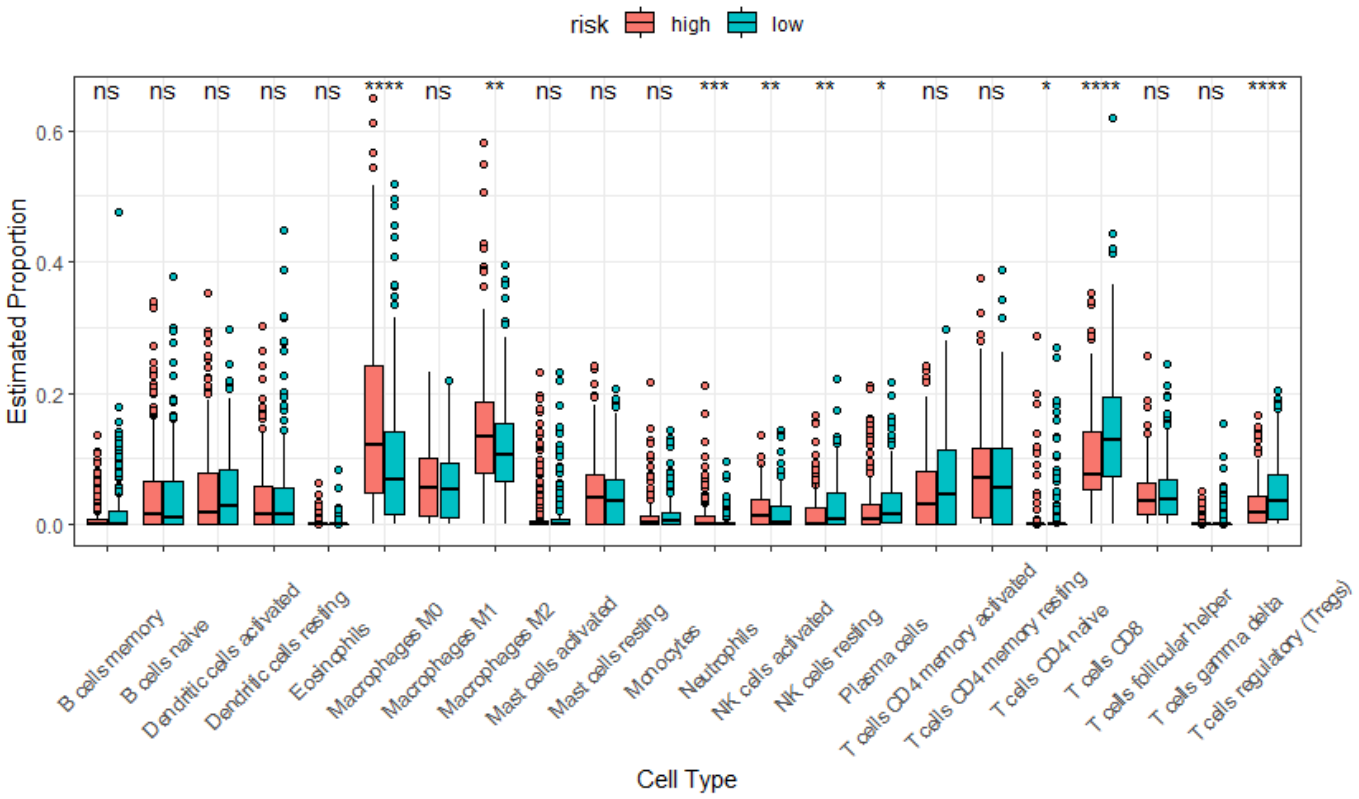

Figure 7

The boxplots showed that 22 immune cells content in the high-risk and low-risk groups (c). *P < 0.05; **P < 0.01; *** P < 0.001; ns: no significance.

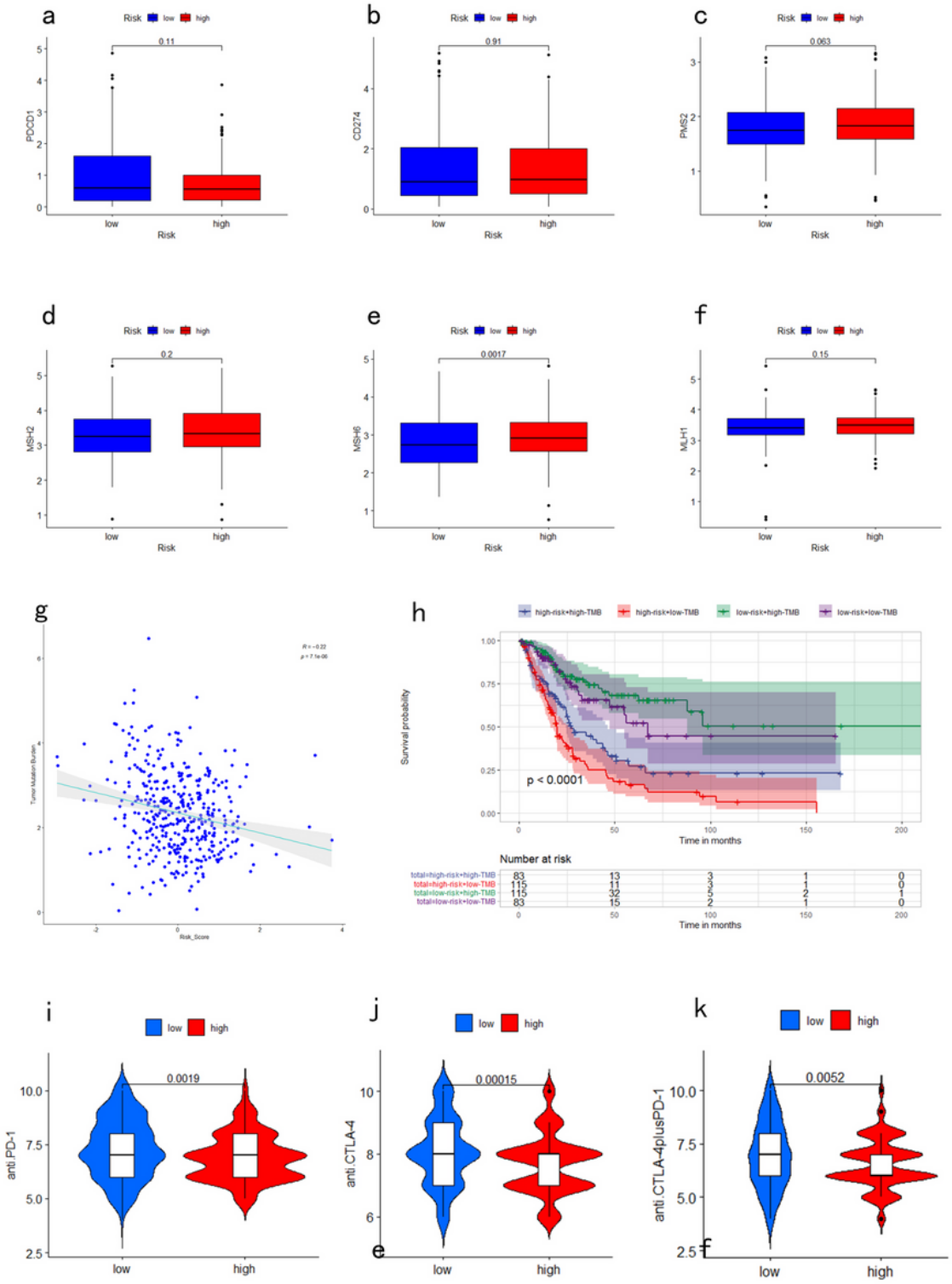

Figure 8

Prediction of immunotherapy response. The expressions of PD-1 and PD-L1 were not significant difference with P > 0.05 (a and b). The expression of mismatch repair genes in tumor samples, MSH2(d), MLH1 (f), were slightly higher in the high-risk group with P > 0.05, while MSH6 (e), and PMS2 (f) expressed significantly higher in the high-risk group. Moreover, with the increment of risk scores, TMB decreased slightly with R =−0.22 and P <0.0001 (g) and the Kaplan–Meier curves showed that patients

with higher TMB and low-risk scores tended to have the best overall survival and those with low TMB and high-risk scores usually had the worst survival probabilities (h). The IPS of anti-PD-1(i), anti-CTLA-4 (j), and anti-(CTLA-4 plus PD-1) (k) in the high-risk group was significant lower than that in the low-risk group, predicting that patients with higher risk scores had a worse immunotherapy response. TMB, tumor mutational burden.

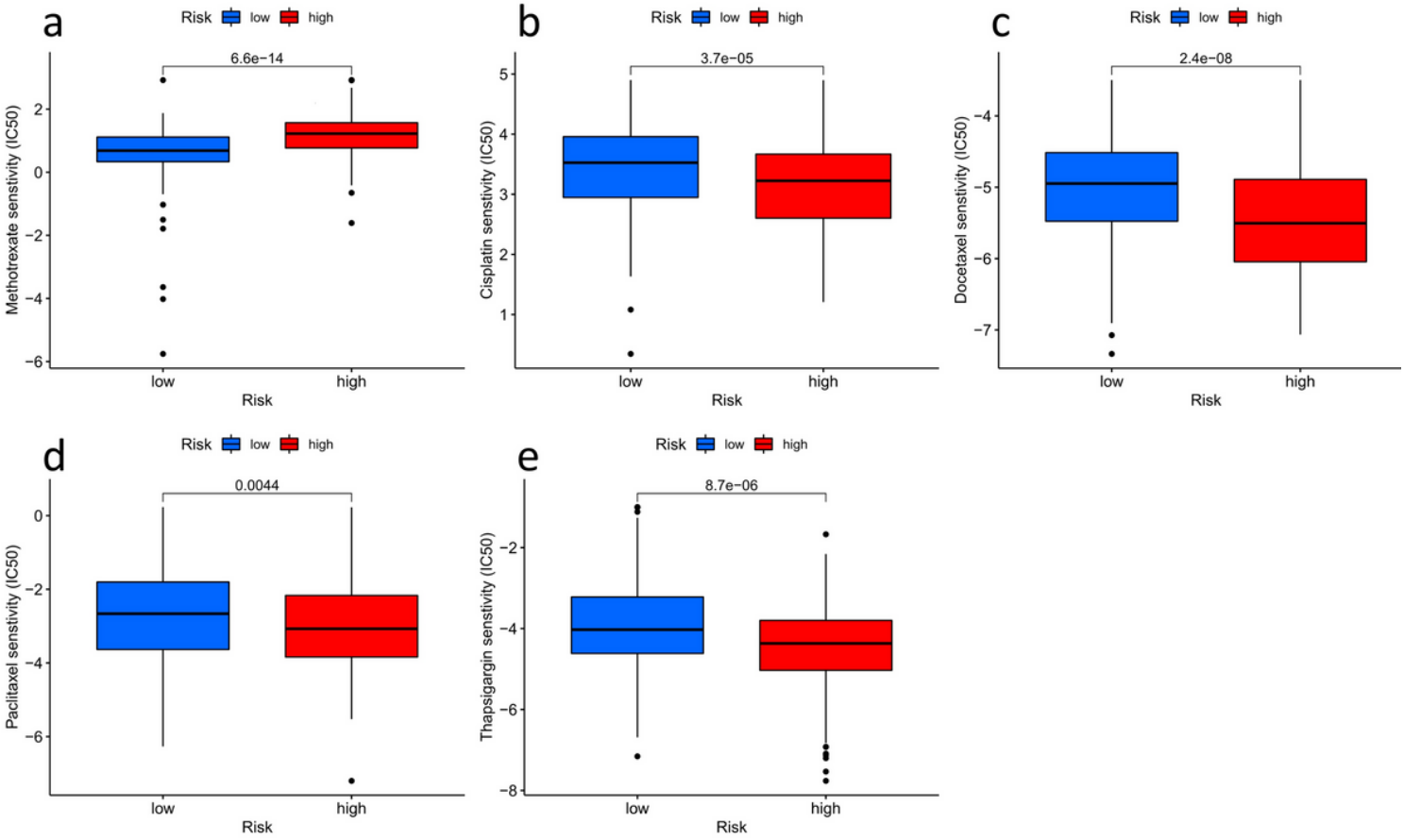

Figure 9

Prediction of chemotherapy response. IC50 of methotrexate (a) in the high-risk group were significantly higher than that in the low-risk group. On the contrary, IC50 of cisplatin (b), docetaxel (c), and paclitaxel (d) and thapsigargin (e) were high in the low-risk group. IC50, half maximal inhibitory concentration.

Supplementary Files

This is a list of supplementary files associated with this preprint. Click to download.

- supplementary.zip